ACS APPLIED MATERIALS & INTERFACES

Research Article

www.acsami.org

Mobility-Enhancing Coatings for Vitreoretinal Surgical Devices: Hydrophilic and Enzymatic Coatings Investigated by Microrheology

Juho Pokki,[*,†] Jemish Parmar,[†] Olgaç Ergeneman,[†] Hamdi Torun,[‡,∥] Miguel Guerrero,[§] Eva Pellicer,[§] Jordi Sort,[§,⊥] Salvador Pané,[*,†] and Bradley J. Nelson[†]

[†]Institute of Robotics and Intelligent Systems, ETH Zurich, Zurich, Switzerland

[‡]Department of Electrical and Electronics Engineering, Boğaziçi University, Istanbul, Turkey

[§]Departament de Física, Universitat Autònoma de Barcelona, Bellaterra, Spain

[∥]Center for Life Sciences and Technologies, Boğaziçi University, Istanbul, Turkey

[⊥]Institució Catalana de Recerca i Estudis Avançats (ICREA), Barcelona, Spain

Supporting Information

ABSTRACT: Ophthalmic wireless microrobots are proposed for minimally invasive vitreoretinal surgery. Devices in the vitreous experience nonlinear mobility as a result of the complex mechanical properties of the vitreous and its interaction with the devices. A microdevice that will minimize its interaction with the macromolecules of the vitreous (i.e., mainly hyaluronan (HA) and collagen) can be utilized for ophthalmic surgeries. Although a few studies on the interactions between the vitreous and microdevices exist, there is no literature on the influence of coatings on these interactions. This paper presents how coatings on devices affect mobility in the vitreous. Surgical catheters in the vasculature use hydrophilic polymer coatings that reduce biomolecular absorption and enhance mobility. In this work such polymers, polyvinylpyrrolidone (PVP), polyethylene glycol (PEG), and HA coatings were utilized, and their effects on mobility in the vitreous were characterized. Hydrophilic titanium dioxide (TiO_2) coating was also developed and characterized. Collagenase and hyaluronidase enzymes were coated on probes' surfaces with a view to enhancing their mobility by enzymatic digestion of the collagen and HA of the vitreous, respectively. To model the human vitreous, ex vivo porcine vitreous and collagen were used. For studying the effects of hyaluronidase, the vitreous and HA were used. The hydrophilic and enzymatic coatings were characterized by oscillatory magnetic microrheology. The statistical significance of the mean relative displacements (i.e., mobility) of the coated probes with respect to control probes was assessed. All studied hydrophilic coatings improve mobility, except for HA which decreases mobility potentially due to bonding with vitreal macromolecules. TiO_2 coating improves mobility in collagen by 28.3% and in the vitreous by 15.4%. PEG and PVP coatings improve mobility in collagen by 19.4 and by 39.6%, respectively, but their improvement in the vitreous is insignificant at a 95% confidence level (CL). HA coating affects mobility by reducing it in collagen by 35.6% (statistically significant) and in the vitreous by 16.8% (insignificant change at 95% CL). The coatings cause similar effects in collagen and in the vitreous. However, the effects are lower in the vitreous, which can be due to a lower concentration of collagen in the vitreous than in the prepared collagen samples. The coatings based on enzymatic activity increase mobility (i.e., >40% after 15 min experiments in the vitreous models) more than the hydrophilic coatings based on physicochemical interactions. However, the enzymes have time-dependent effects, and they dissolve from the probe surface with time. The presented results are useful for researchers and companies developing ophthalmic devices. They also pave the way to understanding how to adjust mobility of a microdevice in a complex fluid by choice of an appropriate coating.

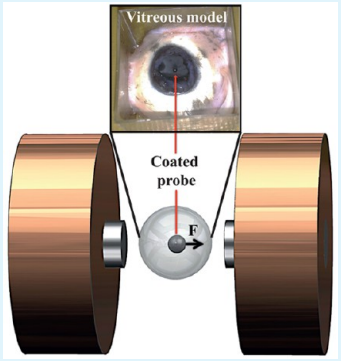

KEYWORDS: *ophthalmic instruments, microrobots, microrheology, coatings, and enzymes*

INTRODUCTION

A variety of ophthalmic diseases[1−3] and traumas[4] lead to reduced living quality and blindness. Age-related macular degeneration (AMD) in the posterior segment of the eye is one of the leading causes of vision loss around the world. In the United States, 1.8 million people suffer from a severe form of the disease (wet AMD), a number projected to reach 3 million in 2020.[5,6] Furthermore, diabetic retinopathy (DR), with its vision threatening form (VTDR), also occurs in the posterior segment of the eye. Its prevalence is expected to triple in the United States (i.e., from 5.5 million patients in 2005 to 16 million patients in 2050 concerning DR; from 1.2 million patients to 3.4 million patients concerning VTDR).[6]

Severe ophthalmic conditions, such as AMD and VTDR, require invasive procedures in the proximity of the vitreoretinal interface, which separates the vitreous body and the retina with

Received: July 30, 2015
Accepted: September 11, 2015
Published: September 11, 2015

DOI: 10.1021/acsami.5b06937
ACS Appl. Mater. Interfaces 2015, 7, 22018−22028

light-sensitive tissue layers. The vitreous is a transparent gel that supports the surrounding eye structures. It is typically removed adjacent to these procedures with pars plana vitrectomy, where the vitreous is cut, aspirated, and replaced by either a fluidic substitute or gas. As retinal complications can arise, alternative procedures are under investigation. To reduce the risk of the vitrectomy complications caused by surgical instruments, pharmacologic vitreolysis using an enzyme called Ocriplasmin,[7] which digests the vitreous, have been developed (FDA approval in 2012).

Ophthalmic microrobots[8] are proposed for minimally invasive procedures in the eye, used ideally without a vitrectomy. Untethered microdevices can also access parts of the eye that are difficult to reach with conventional surgical tools. Operation of such devices or new vitrectomy instruments in contact with the vitreous face challenges regarding nonlinear mobility (i.e., viscoelastic interaction[9,10]) and biomolecular adsorption,[11,12] which hinder the movement and involve the risk of complications.

The viscoelastic interaction is a consequence of molecular structures of the vitreous (i.e., HA and the collagen fiber network)[9] responding to the stresses applied by surgical devices. The 3D spatial arrangement of these molecular structures affects how they interact with the devices.[11] Therefore, coatings on the devices, in addition to their geometry[13] and dimensions,[14] may allow for modifications of the viscoelastic interaction. The effects of functionalized coatings on the mobility of 1 μm diameter probes have been studied in F-actine fibrous models using passive microrheology.[12] Hydrophilic coatings[15] have been successfully used on catheters to reduce biomolecular adsorption and to enhance mobility in the vasculature. No literature, however, exists on the effect of hydrophilic coatings on the mobility of devices in the vitreous. There are also no studies on investigating the effects of enzyme-coated devices on the mobility in the vitreous.

In this work, hydrophilic and enzymatic coatings on 1 mm-diameter probes (modeling surgical devices) were investigated for their effects on mobility. Ex vivo porcine vitreous, a standard model of the human vitreous, was used. To model potentially biofouling/adsorbing macromolecular structures of the vitreous, synthesized collagen gel (type I) was used. Four different biocompatible hydrophilic coatings on probe surfaces were used. The coatings for this study were chosen on the basis of their minimal protein adsorption properties, which in turn, can improve mobility: previous reports show how protein adsorption is mainly governed by hydrophobic interactions.[16] Hydrophilic coatings were reported to minimize protein adsorption, thus we considered them the most suitable for studying how to enhance mobility of devices using functional coatings. Three hydrophilic coatings, PVP, PEG, and HA, were prepared using the method described by Serrano et al.[15] The fourth coating, TiO_2, was prepared using an optimized sol–gel method. Two enzymes, collagenase to digest collagen and hyaluronidase to digest HA, were covalently immobilized on the probes. The coatings were characterized by scanning electron microscopy (SEM), high-resolution transmission electron microscopy (HRTEM), fluorescence microscopy, ellipsometry, and energy-dispersive X-ray spectroscopy (EDX). The effect of the probe's coating on mobility in the vitreous was studied using oscillatory magnetic microrheology. The time-independent effects of the hydrophilic coatings and the time-dependent effects of the enzyme coatings were characterized. The microrheological system, developed and optimized to characterize the effects of coatings on probe mobility relevant for microrobots and ophthalmic surgical instruments, is based on methods that have been widely used.[17] From the relative variation of the rheological parameters, the differences of coatings can be quantified. Spherical probes are commonly used in microrheology[17] because they allow for symmetric distribution of stresses and straightforward calculations. The viscoelastic interaction influencing spherical probes relates to the influence in probes with different shapes[13] that robotic vitreoretinal devices in a surgery can have. The size of the probe was chosen comparable to the devices for ophthalmic surgery (i.e., for vitrectomy[18]). The probe excitation frequencies (0.5–5 Hz) include the relevant frequencies corresponding to the relaxation time scales of the collagen fibers (approximately 1 s)[9] most relevant to potential biofouling.

MATERIALS

Spherical, hard-magnetic 1 mm diameter probes (neodymium iron boron N45 balls, remanence 1.33–1.36 T; Dortmund, EarthMag GmbH) were used in all experiments for studying mobility in the vitreous. The probes were coated with four hydrophilic coatings and with two covalently immobilized enzymes. The probes were inserted into vitreous models, as shown in Figure 1.

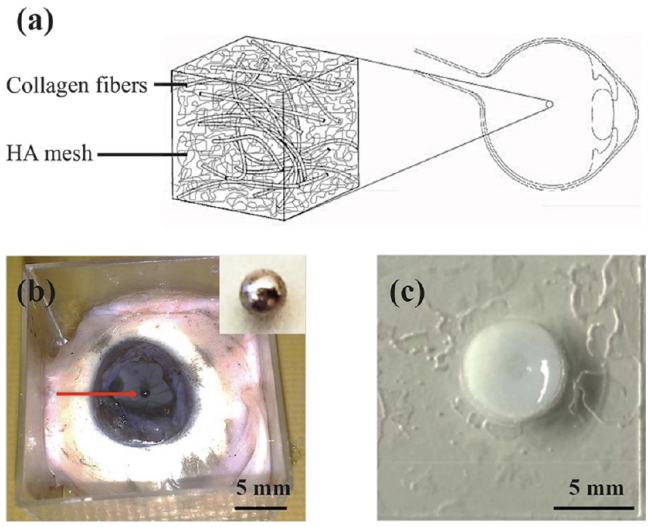

Figure 1. (a) An illustration of the vitreous consisting of collagen fibers and HA. (b) Ex vivo porcine eye and (c) collagen gel. Access to the vitreous, seen in panel b, was gained by first removing the cornea, lens, and iris of the eye. The probe denoted with a red arrow, was inserted in the central part of the vitreous. The inset in panel b shows the 1 mm diameter probe used in the experiments with the vitreous and collagen. Probes were inserted in the (c) collagen gel so that they were >2 mm from the walls of the holder and from the surface. The diameter of the holder, as well as its thickness, were 6 mm.

Table 1. Polymer Solutions for Coatings

polymer	solvent	concn (mg/mL)
HA	water	17.6
PVP	ethanol	0.3
PEG	water	0.1

DOI: 10.1021/acsami.5b06937
ACS Appl. Mater. Interfaces 2015, 7, 22018–22028

Table 2. Water Drop Contact Angle on Hydrophilic Polymer Coatings

polymer coating	contact angle (deg)
HA	12.5 ± 1.3
PVP	13.2 ± 0.7
PEG	15.3 ± 1.6
TiO_2	40.9 ± 2.1

Vitreous Models. Ex vivo porcine vitreous, and a collagen/HA gel were used to model the biomechanical behavior of the human vitreous and its main macromolecules (Figure 1a), respectively. Ex vivo porcine vitreous (Figure 1b) is a standard model used to mimic the anatomical, chemical, and mechanical properties of the human vitreous.[9,19,20] Fresh porcine eyes were purchased from a local abattoir in Zurich and then maintained in a refrigerator at 5 °C prior to the experiments (maximum storage 12 h). Each eye was dissected to remove the cornea, lens, and iris, which allowed a direct optical access to the vitreous.

The collagen fibers in the vitreous that have a concentration of around 300 μg/mL[21] form a highly organized structure (collagen type II fibers connected with collagen fiber types V/XI and IX).[22] To model the collagen fibers, we prepared collagen gel from type I that is widely used as a standard stabile scaffold biomaterial (e.g., in tissue engineering).[23] It is challenging to reproducibly synthesize gels of other types of collagen fibers due to inadequate chemical stability. This synthesized collagen gel aims to possess the effects of a fibrous environment, the relevant chemistry of the fibers, and the contact of the fibers with the probe (guaranteed by an adequate concentration of collagen). During the synthesis, various parameters can be tuned for optimal polymerization; concentration of the collagen solution, pH, ion strength, and temperature affect the dynamics of polymerization.[24] For 400 μL of collagen (from rat tail, Corning, cat. no. 354249) that was prepared for each microrheology experiment, 10.4 μL of 0.1 M NaOH was used to neutralize the collagen. A concentration of 5 mg/mL was used to ensure the mechanical contact between

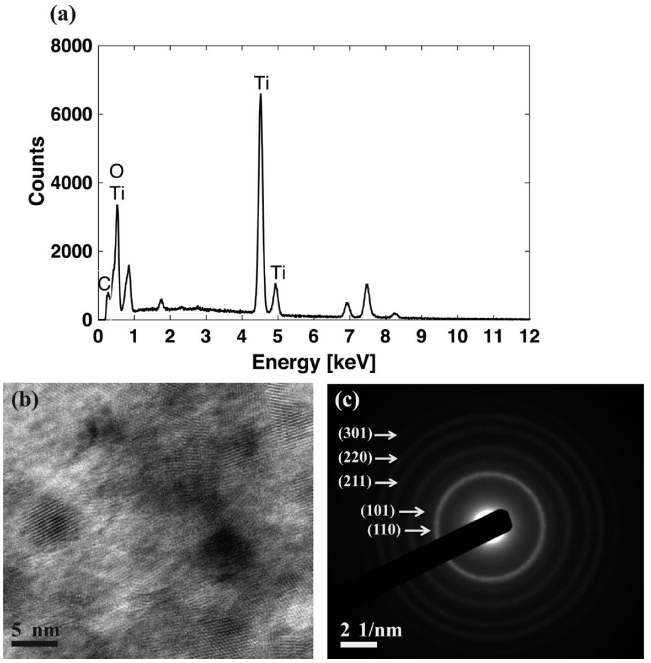

Figure 3. (a) Sol–gel-coated TiO_2 surface analyzed by EDX. (b) HRTEM of TiO_2. (c) Lattice fringes corresponding to (110), (101), (211), (220), and (301) are due to TiO_2 anatase nanocrystals.

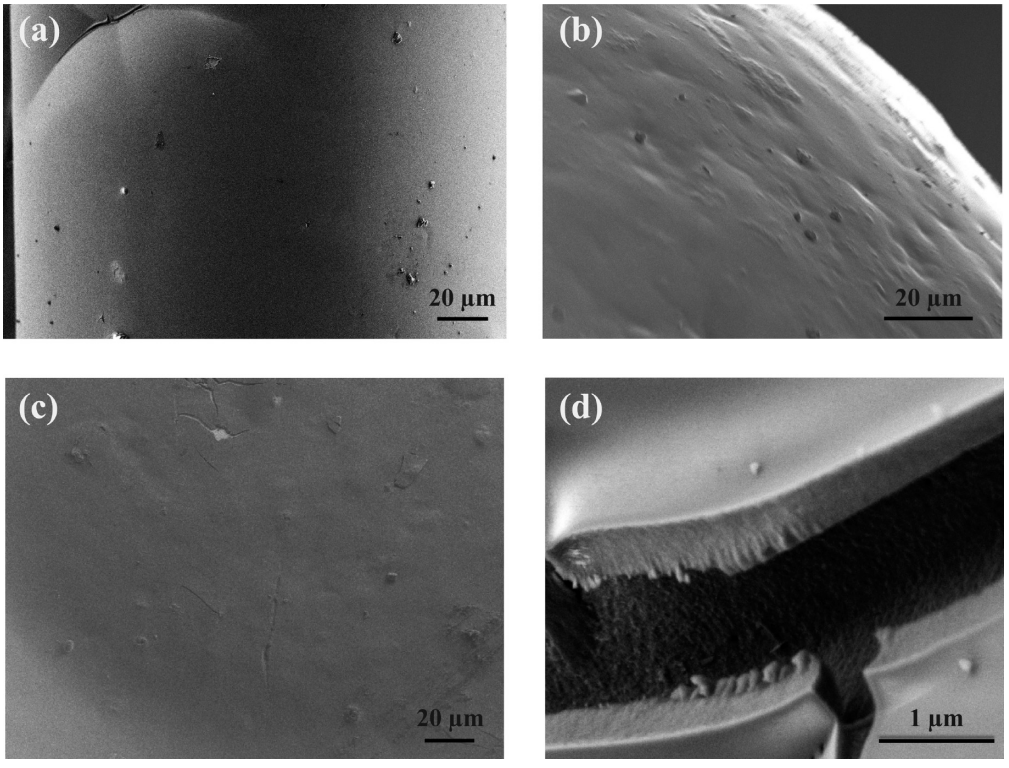

Figure 2. (a) SEM images from a sol–gel-coated TiO_2 surface on a custom-made cylinder on which the coating method was initially developed. (b and c) SEM images of the optimized TiO_2 coating on a spherical probe. (d) Cross-sectional view of a crack.

DOI: 10.1021/acsami.5b06937
ACS Appl. Mater. Interfaces 2015, 7, 22018–22028

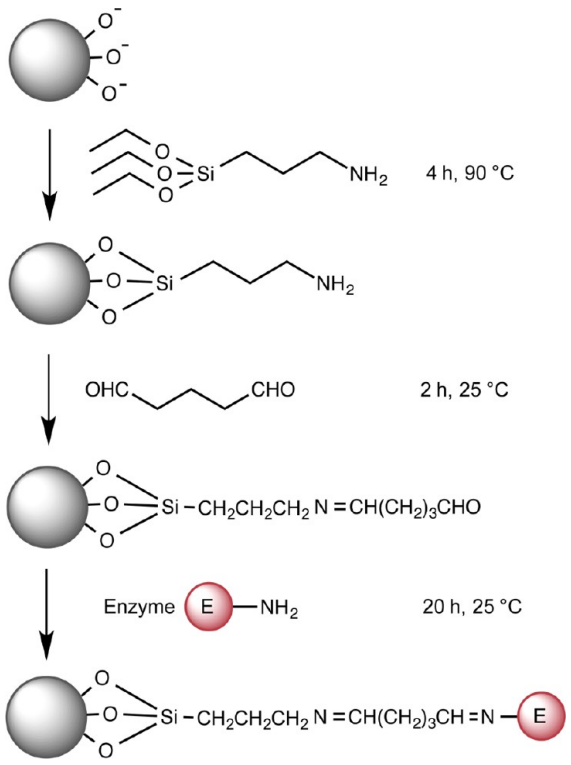

Figure 4. A schematic illustration of reaction steps involved in immobilizing an enzymatic coating.

experimental probes and the collagen. This concentration was further used to prepare a stable gel, as collagen in lower concentrations takes longer to polymerize and remains less stable.[24] The prepared solution was first transferred to a container made for the microrheology experiments. The collagen solution was then allowed to polymerize for 20 min at room temperature prior to the experiments. Figure 1c shows a collagen gel sample after polymerization. The polymerization time was characterized with a similar principle used by Nickerson et al.[24] As the polymerization progresses, collagen fibers start to develop. They diffuse light, thus transmission decreases and the gel becomes opaque. The decrease in transmission is directly related to the intensity of the images recorded by camera. The average intensity plotted against time is shown in the Supporting Information (Figure S1). The obtained data agree well with the polymerization results in the literature.[24]

To study the effects of hyalurodinase enzyme on vitreal mobility, we prepared HA gel. Commercially available dry lyophilized powder state HA (Sigma-Aldrich, CAS 9067-32-7, SKU 53747) was mixed with DI water to form an aqueous solution. Human vitreous has a HA concentration of 0.1−0.2 mg/mL for 10- to 60-year-old individuals, whereas the concentration increases for 70-year-old individuals.[25] A larger concentration of HA (5 mg/mL) was used in this model to guarantee the interaction of HA with the coated probes.

Hydrophilic Coatings Prepared on Probes. Four coatings, polyvinylpyrrolidone (PVP), polyethylene glycol (PEG), hyaluronan (HA), and titanium dioxide (TiO_2) were prepared on probes to characterize their effects to mobility. Minimal protein adsorption can help enhance probe mobility in the vitreous models. PVP and PEG coatings have been studied for protein adsorption using methods involving variable-angle spectroscopic ellipsometry (VASE) and quartz-crystal microbalance with dissipation (QCM-D).[15] The work of Serrano et al.[15] reports minimal protein adsorption for both coatings with reference to SiO_2 surface. PVP and PEG coatings have also been studied for their short-term stability in contact with salt water (i.e., PVP had an average removal rate of 0.2 nm/h, while PEG had 2.2 nm/h).[15] The preparation of PVP, PEG, and HA is based on a coating protocol developed by Serrano et al.[15] Briefly, an adhesion promoter polyallylamine-grafted-perfluorophenylazide (PFPA-*g*-PAAm) solution was produced from polyallylamine (PAAm) and perfluorophenylazide (PFPA). It was diluted using a solution of ethanol and 4-(2-hydroxyethyl)-1-piperazineethanesulfonic acid (ethanol-HEPES1) solution with a volume ratio of 3:2. After that, the probes were cleaned and treated with oxygen plasma to modify the negatively charged surface, which is required for application of the adhesion promotor PFPA-*g*-PAAm. The probes were immersed in PFPA-*g*-PAAm solution for 30 min, then rinsed with 3:2 ethanol-HEPES1, and subsequently with DI water. The probes were then dipped in the polymer solution and allowed to dry for 15 min. Table 1 shows the polymer solutions with their concentrations required to prepare PVP, PEG, and HA. All the probes were then exposed to UV light with a 254 nm wavelength for 2 min. Upon activation with UV light, the azide group of the PFPA-*g*-PAAm adhesion promoter covalently binds with the carbon/nitrogen atoms of each of the hydrophilic polymers.[15] Finally, the probes were immersed in the solvent (the solvent for each polymer is shown in Table 1), so that the unbound and surface-adsorbed polymer was removed from the surface.

The fourth hydrophilic coating, TiO_2, is a suitable coating candidate for bioapplications because it enhances biocompatibility regardless of dimension, size, or crystal structure. No significant effects on the morphology or oxidative stress level of cells have been found.[26] The sol−gel method has been used by many researchers to synthesize TiO_2 nanoparticles and coatings.[27,28] The TiO_2 coating was prepared using a PEG-modified sol−gel process. The PEG modification yields anatase TiO_2[29] at temperatures as low as 80 °C and also enhances biocompatibility.[30] Titanium(IV) butoxide (TBO) (Sigma-Aldrich, cat. no. 244112) was used as a primary TiO_2 precursor, which was added to ethanol. Subsequently HCl and PEG was added to the mixer, and water was added last. HCl was used as a catalyst for hydrolysis reaction and PEG helped to stabilize TiO_2 colloids.[28] All chemicals were mixed using a vortex mixer. The volume ratio of the prepared solution was TBO/PEG/EtOH/H_2O/HCl = 1:1:9:0.15:0.01. The solution was kept overnight, and the next day, the probes were coated by dip-coating using a micro manipulator (MP-285, Sutter instruments). A total of three dipping cycles were performed, and the probes were then kept in an oven at 80 °C for 1 h.

Contact angle was measured from coatings prepared on flat chips (silicon [100] with 6 nm gold for adhesion). Table 2 shows the contact angles from PVP, PEG, HA, and TiO_2 coated on the chips. The thickness of the PVP coating was measured by ellipsometry (M-2000FTM spectroscopic ellipsometer, J.A. Woollam Co.). The thicknesses of the other coatings, PEG and HA, are comparable to the PVP. The measured adhesion promoter (PFPA−PAAm) thickness was 1.77 ± 0.10 nm while the thickness of PVP on top of adhesion promoter was 8.34 ± 0.45 nm. The total measured thickness of the coating was 10.11 ± 0.37 nm. As a newly developed coating, the TiO_2 coating needed further characterization. SEM observation revealed

DOI: 10.1021/acsami.5b06937
ACS Appl. Mater. Interfaces 2015, 7, 22018−22028

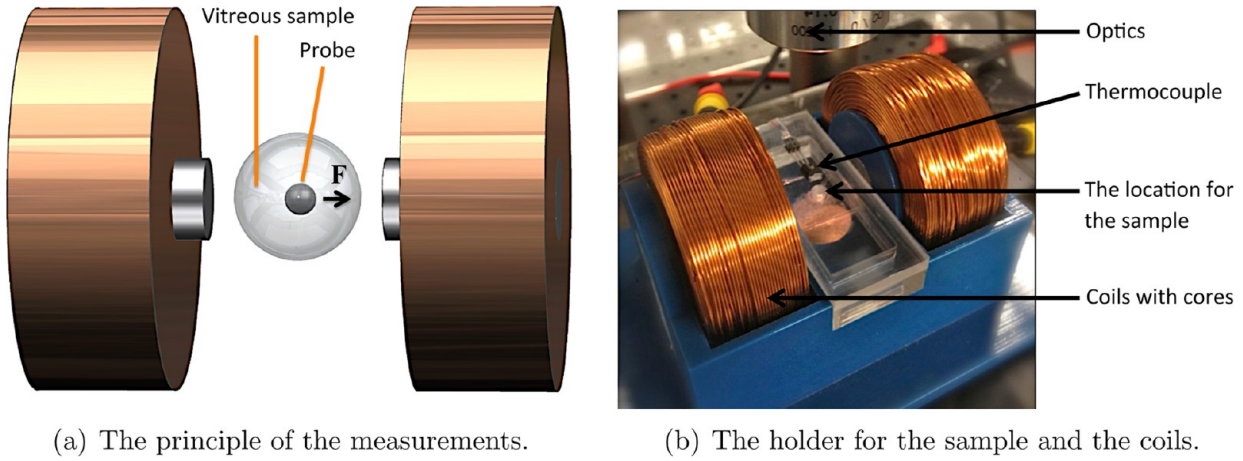

(a) The principle of the measurements. (b) The holder for the sample and the coils.

Figure 5. (a) A probe is used to perform measurements in a vitreous sample. Force F was applied on the probe. (b) The samples were centered between two magnetic coils on a 3D printed holder. The coil inner diameter is 13.5 mm (fitting a core with a diameter of 13.5 mm), outer diameter is 60 mm and length is 27 mm. The copper wire diameter is 0.71 mm. A high-speed camera attached to the optics was used to track the probe. The photo is a mirror image that is used for clarity.

TiO_2 surfaces (Figure 2a–c) that were homogeneous and having only some cracks of a few micrometers within a range of hundreds of micrometers. Some cracks are due to inhomogeneity of the surface on which the coating was applied. The thickness of the TiO_2 coating was approximately 0.5 μm (see a cross-sectional view of a crack in Figure 2d). The TiO_2 coating was characterized with EDX (Figure 3a) to detect the presence of Ti and O elements within the coated surface. Figure 3b shows a HRTEM image of a specimen coated with TiO_2. The HRTEM results with selected area diffraction confirmed that TiO_2 was present in anatase nanocrystalline form (see diffuse rings in Figure 3c).

Enzyme Coatings Prepared on Probes. Collagenase and hyaluronidase enzymes were prepared on the probe surfaces using irreversible enzyme immobilization using a method developed by Nanci et al.[31] It is not possible to detach the enzymes from the surface without destroying enzyme activity or the surface to which the enzyme is attached.[32,33] The TiO_2 coating was first prepared on the probe surface according to the protocol depicted. TiO_2 layer not only renders biocompatibility to the devices but also enables covalent immobilization of the enzymes on its surface required for preparing robust enzymatic coatings controllably. The prepared TiO_2 surface was cleaned using acetone and toluene. Figure 4 shows a schematic of the reaction steps involved in the enzyme immobilization. The probes were immersed in a (3-aminopropyl)triethoxysilane solution (Sigma-Aldrich, cat. no. 440140) diluted to 10% with toluene. They were kept in the solution preheated to 90 °C for 4 h. After removing from the solution, the probes were rinsed with toluene and with DI water. In the next step, the probes were immersed in a 1% glutaraldehyde solution (Sigma-Aldrich, cat. no. G5882) at 25 °C for 2 h. Finally, the surfaces were rinsed with DI water. Glutaraldehyde becomes fluorescent when reacting with amine groups of (3-aminopropyl)-triethoxysilane. The presence of (3-aminopropyl)-triethoxysilane-linked glutaraldehyde on the probe (i.e., serving as an adhesion layer for covalent immobilization of enzymes) was confirmed by observing fluorescence on the probe surface. Two enzyme coatings, collagenase (from *Clostridium histolyticum*, Sigma-Aldrich, cat. no. C7657) and hyaluronidase (from bovine testes, Sigma-Aldrich, cat. no. H3631), were prepared. The probes were immersed in 2 mg/mL aqueous solution of the enzyme at room temperature overnight.

METHODS

Setup for Oscillatory Microrheology. A custom-built magnetic microrheometer was used to study the effects of the coatings on probe mobility. Figure 5a illustrates the principle of using a magnetically actuated coated probe in the experiments. A magnetic force is applied on the probe by magnetic field gradients. The 3D-printed sample and electromagnet holder is shown in Figure 5b. It has a workspace for vitreous samples between two electromagnetic coils (Coil 1 and Coil 2; Trafomic, Raisio, Finland) with cobalt–iron cores (Vacoflux 50, Vacuumschmelze, Hanau, Germany). The setup maintains a core-to-core separation at 28 mm to fit an ex vivo porcine eye in the workspace. Each coil is connected to a power amplifier (AE Techron 7224). Labview-based software is used to generate and control sinusoidal voltage signals fed to a DAQ board (National Instruments, NI 6229), which is output to the amplifiers driving the coils. The software records the currents fed through the coils that correspond with magnetic fields and field gradients. Magnetic fields are generated using currents $i_{\text{Coil 1}}$ and $i_{\text{Coil 2}}$ fed to Coil 1 and Coil 2, respectively. The relationship of the currents to magnetic fields is linearly proportional within the range of the applied fields (0A–5A). The currents $i_{\text{Coil 1}}$ and $i_{\text{Coil 2}}$ are as follows:

$$i_{\text{Coil1}} = i_{\text{gradient}} + i_{\text{field}},\ i_{\text{Coil2}} = -i_{\text{gradient}} + i_{\text{field}} \quad (1)$$

where the currents to generate gradients (i_{gradient}) and fields (i_{field}) are superpositioned. The gradient is generated by applying a spatially varying field (B_{gradient} (p; i_{gradient})). The gradient is then superpositioned with a field offset (B_{field} (i_{field})):

$$B(p;\ i_{\text{gradient}},\ i_{\text{field}}) = B_{\text{gradient}}(p;\ i_{\text{gradient}}) + B_{\text{field}}(i_{\text{field}}) \quad (2)$$

Table 3. Force Values Used in the Experiments[a]

vitreous model	magnetic force (10^{-6} N)
ex vivo porcine vitreous	8.4
collagen gel	168
HA gel	168

[a]The force amplitude was chosen for moving the probe approximately one body length. Remark: the movement in collagen and HA gel needed 20 times more force than in ex vivo porcine vitreous.

DOI: 10.1021/acsami.5b06937
ACS Appl. Mater. Interfaces 2015, 7, 22018–22028

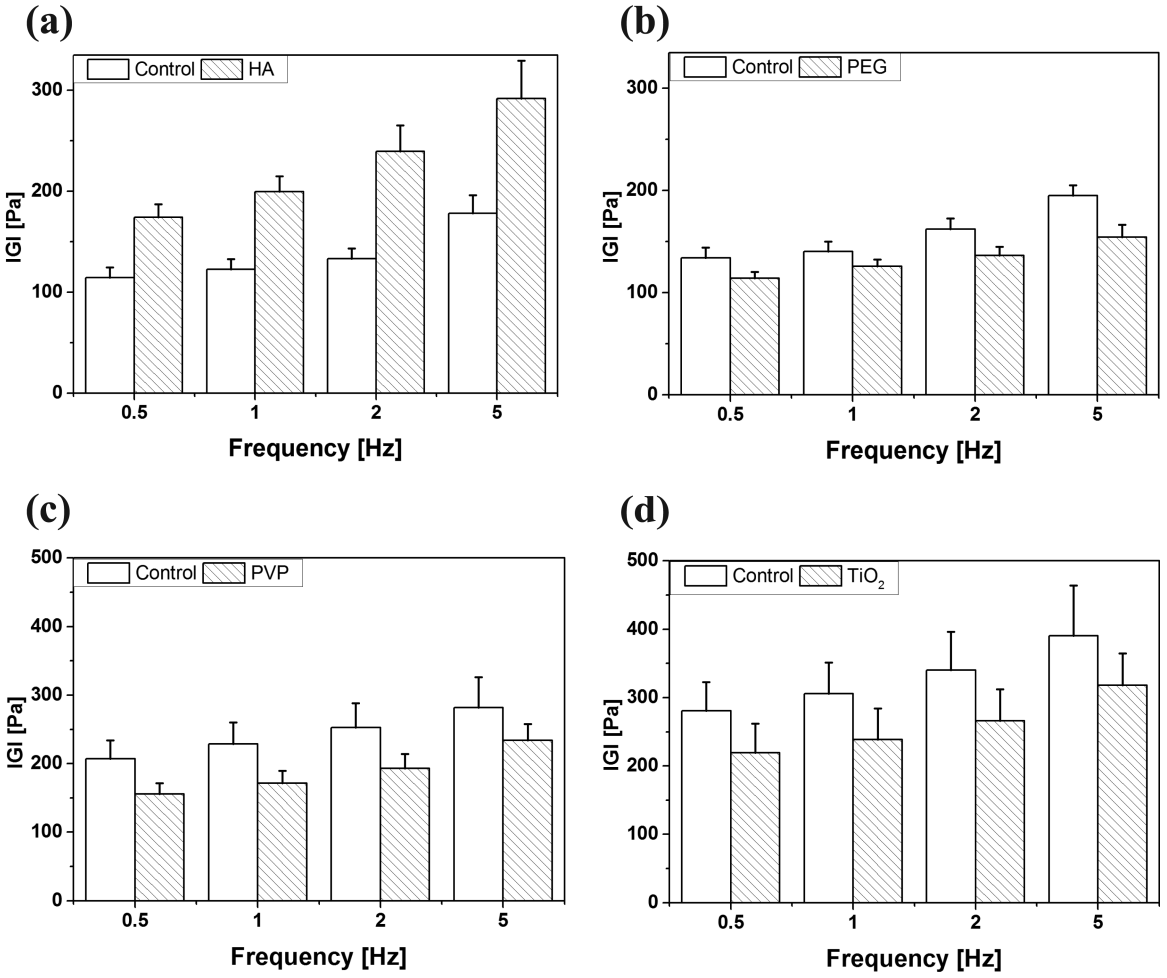

Figure 6. Mean |G| values measured in collagen gel by probes coated with (a) HA (n = 4), (b) PEG (n = 3), (c) PVP (n = 5), and (d) TiO_2 (n = 3) are shown. The SeM values are in error bars.

where B (T) is spatially varying magnetic field applied on the probe and $p = [x\ y\ z]$ is the position of the probe. The coordinate x in horizontal plane gives the axial (on-axis) position between Coils 1 and 2. The coordinates y in horizontal plane and z in vertical plane give the off-axis position. Magnetic force ($F_{magnetic}$) applied by the system on the probe is

$$F_{magnetic} = \left[\frac{\partial B}{\partial x}\frac{\partial B}{\partial y}\frac{\partial B}{\partial z}\right]^{T} M(B)V \tag{3}$$

where M (A m^{-1}) is the magnetization of the probe, and V (m^3) is the volume of the probe. A gradient $\frac{\partial B}{\partial x}$ is applied at axial direction by varying $i_{gradient}$. The components $\frac{\partial B}{\partial y}$ and $\frac{\partial B}{\partial z}$ are minimized in the center of the magnetic workspace. Magnetic fields (Supporting Information, Figure S2) from the coils were characterized by a magnetometer (Metrolab THM1176), mounted on a 3D micromanipulator (SmarAct MCS-3D). At the center, the gradient was 3.0 $\frac{T}{m}$ at $i_{gradient}$ = 1 A. The magnetic fields and gradient inhomogeneity were also simulated using Comsol, as shown in Figure S2. The applied current values in the simulation were corrected to take into account the construction of the coils (i.e., the fill factor in the winding). The magnetization (M) direction of the probe is maintained by applying a field offset B_{field} (i_{field}). Changing field direction (see Figure S2a; k = 0) rotates the probe. A unidirectional B_{field} (i_{field}) is used, when sinusoidal gradients are applied on a probe, located within 1 mm from the center of magnetic workspace. B_{field} (i_{field}) is set based on proportionality factor k and the current amplitude corresponding the oscillatory gradients $\frac{\partial B}{\partial x}(\hat{i}_{gradient})$:

$$i_{field} = k\hat{i}_{gradient} \tag{4}$$

The effect of k is shown in Figure S2a. The values k = 0, and k = 0.3 are shown for field measurements and the Comsol simulation. Figure S2b shows the effects of k to gradient variation around the center of the magnetic workspace in an axial direction. There is a 7.0% (at k = 0.3) variation of the gradients $\frac{\partial B}{\partial x}$ within 1 mm around the center of the magnetic workspace. A high-speed camera (Optronis CamRecord CL600 × 2) connected to optics (Mitutoyo MT-4 tube lens with Mitutoyo Plan Apo 5× objective, NA = 0.14, resolving power 2.2 μm with green light λ = 0.5 μm) is mounted above the magnetic workspace in order to record the displacement of the probe. The pixel-to-micrometer conversion of the system is 2.80 μm/pix. The camera is triggered by a signal from the DAQ, which is controlled utilizing the same LabView software used to apply the sinusoidal magnetic fields.

Protocol. Each vitreous sample was placed in the center of the magnetic workspace. A sinusoidal force with a defined amplitude (Table 3) was applied on a probe to study the effect of the coating in a vitreous sample. Four frequencies with the sinusoidal forces were applied in each experiment: 0.5, 1, 2, and 5 Hz. These frequencies were chosen because they are relevant to the collagen network relaxation times reported in the literature.[9] A field offset corresponding to k = 0.3 was applied to always keep the magnetic field in the same direction. For each frequency, images were recorded for 10 s at a camera speed of 100 fps. For the experiments with the coated probes, control

DOI: 10.1021/acsami.5b06937
ACS Appl. Mater. Interfaces 2015, 7, 22018−22028

experiments were performed in similar conditions using uncoated probes. All the measurements were performed at 24−25 °C.

All the hydrophilic coatings and the collagenase enzyme coatings were studied in ex vivo porcine vitreous and in collagen gel models. Hyaluronidase enzyme coating was tested in ex vivo porcine vitreous and in HA gel instead of collagen gel, because the hyaluronidase enzyme is specific to the HA molecules in the vitreous. To study the time-dependent effects of collagenase and hyaluronidase coatings, experiments were repeated at 5 min intervals up to 25 min. The time-dependent experiments were performed at a constant probe excitation frequency (2 Hz).

In the experiments with collagen and HA gel, the probe blocks the light from the light source placed below the workspace. Thus, dark transmission images of the probe were recorded against a bright sample. In the experiments with ex vivo porcine vitreous, the light source was placed above the workspace. Thus, bright reflection images of the probe were recorded against a dark sample.

A Matlab-based image processing algorithm was used to track the position of the probe in each image. The amplitude of the sinusoidal displacement of the probe was extracted and used in further calculations. The effective absolute shear modulus (|G|) and relative displacement (RD) were calculated for coated and control probes to compare mobility. The effective absolute shear modulus is

$$|G| = \frac{F^{\text{amplitude}}}{6\pi r x^{\text{amplitude}}} \tag{5}$$

where $F^{\text{amplitude}}$ is the amplitude of force, r is the radius of the probe, and $x^{\text{amplitude}}$ is the amplitude of the displacement. The relative displacement from each vitreous sample was calculated to be able to combine mobility data from several vitreous samples with individual differences:

$$\text{RD} = \frac{x_{\text{coated}}^{\text{amplitude}}}{x_{\text{control}}^{\text{amplitude}}} \tag{6}$$

where $x_{\text{coated}}^{\text{amplitude}}$ is the displacement amplitude of the coated probe, and $x_{\text{control}}^{\text{amplitude}}$ is the displacement amplitude of the control probe in the same sample as the coated probe. The control probe was an uncoated probe in all measurements, except in the time-dependent measurements for enzymatic coatings. In the time-dependent measurements, the initial displacement amplitude of the coated probe was considered as $x_{\text{control}}^{\text{amplitude}}$. Using the measure of RD minimizes the effects of the individual variation between the vitreous models; therefore, smaller sample sizes yield to adequately accurate results.

An unpaired t test (two tailed) was used for statistical testing of the relative displacement results at 95% CL. Test group results (with coatings) and control group results (without coating) were compared. The results were interpreted based on the calculated p-values of the t test. Bonferroni correction for multiple comparisons was applied to get an adjusted p-value.

Using the t test allows for testing for statistical difference of mobility between the control and test coatings. The null hyphothesis of the t test states that there is no difference between the coatings. P-values provide a measure of statistical significance for rejecting or confirming a hypothesis. To reject the hypothesis, or in other words, to confirm a difference in mobility between two coatings, a p-value below a cutoff is required. A typically used cutoff of 0.05 corresponding to a 95% confidence level is used for p-values. However, there are controversies related to cut-offs of p-values.[34] Therefore, all obtained p-values are reported and the statistical significance can be then evaluated accurately. There is an inherent variation within the vitreous models (ex vivo porcine vitreous, collagen, and hyaluronan). Although the effects of the variation are minimized by using RDs in calculations, a higher confidence level (e.g., 99%) with a smaller cutoff of the p-values could lead to false negative interpretations of significance. Concerning the 95% confidence level we consider:

P-value < 0.05. A particular coating/enzyme was interpreted to improve mobility with two conditions: (1) RD > 1 (i.e., the coated probe moved more than the control probe); (2) the mean |G| of the experiments with coated probes was equal or less than that for the control experiments. A particular coating/enzyme was interpreted to worsen mobility with two conditions: (1) RD < 1 (i.e., the coated probe moved less than the control probe); (2)The mean |G| of the experiments with coated probes was equal or more than that for the control experiments.

P-value ≥ 0.05. A particular coating/enzyme was interpreted to have no significant effect in mobility, if p-value ≥0.05.

RESULTS AND DISCUSSION

The probes coated with hydrophilic coatings and enzymes were characterized for their ability to enhance mobility in the vitreous models. |G| and RD were characterized for every coating. From each sample (i.e., ex vivo porcine eye, collagen gel and HA gel samples), at least five sets of data were recorded and averaged at each frequency. There were n samples in each coating experiment (i.e., n = 3−8 of collagen gel; n = 3−8 of ex vivo porcine eye vitreous; n = 2−7 of HA gel). The RD results from n samples were validated with the unpaired t test. Mean values of the results with their standard error mean (SeM) are presented. The magnitude and frequency-dependent trend of |G| control measurements in ex vivo porcine vitreous (mean ± SeM: 6.2 ± 1.2 Pa at 0.5 Hz; 6.5 ± 1.3 Pa at 1.0 Hz; 6.9 ± 1.4 Pa at 2.0 Hz; 8.4 ± 1.7 Pa at 5.0 Hz; n = 33) are similar as in literature.[9,11] |G| values vary within an order of magnitude, which is a normal variation between individual vitreous samples. The control experiments in the synthesized collagen gel have similar values as in the literature (mean ± SeM: 179.6 ± 15.2 Pa at 0.5 Hz; 209.0 ± 18.8 Pa at 1.0 Hz; 252.2 ± 24.8 Pa at 2.0 Hz; 335.5 ± 39.0 Pa at 5.0 Hz; n = 30).[35,36] The average

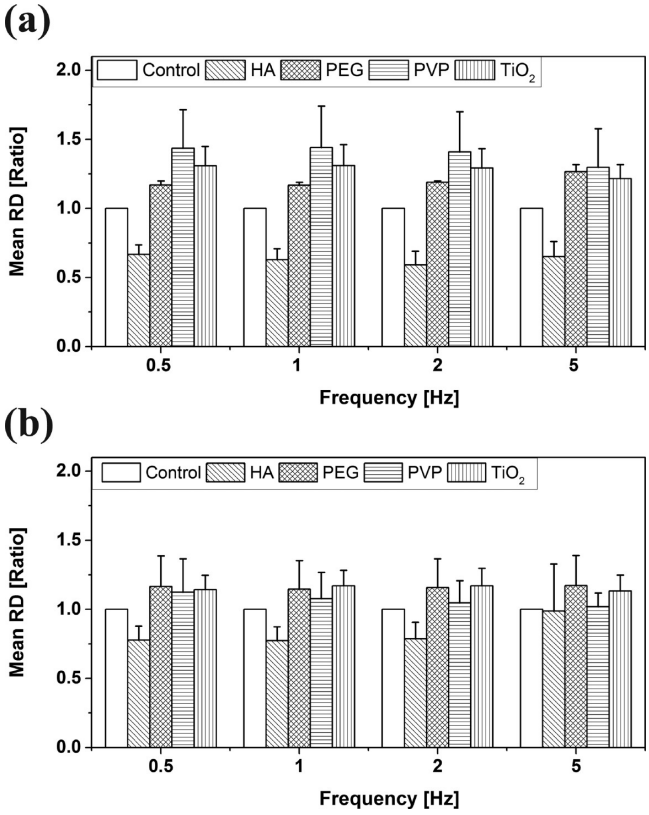

Figure 7. Mean RD values for HA, PEG, PVP, and TiO_2 coatings in (a) collagen gel and (b) ex vivo porcine vitreous. The SeMs are shown in error bars.

DOI: 10.1021/acsami.5b06937
ACS Appl. Mater. Interfaces 2015, 7, 22018−22028

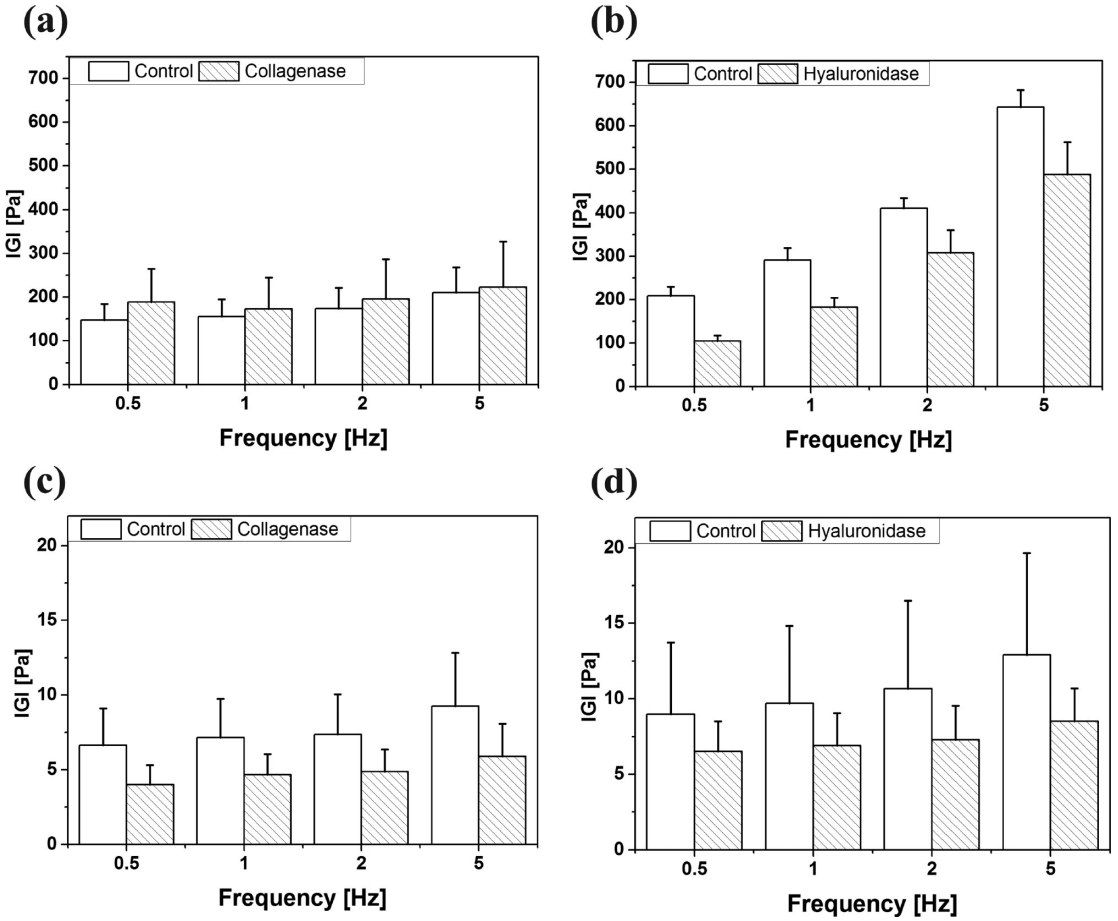

Figure 8. Mean |G| for the collagenase- and hyaluronidase-coated probes. (a) Collagenase-coated probes in collagen gel (n = 8). (b) Hyaluronidase-coated probes in HA (n = 7). (c) Collagenase-coated probes in ex vivo porcine vitreous (n = 8). (d) Hyaluronidase-coated probes in ex vivo porcine vitreous (n = 6).

variation of |G| of the prepared collagen gel samples is less than in the ex vivo porcine vitreous samples.

The shear modulus that describes the viscoelastic interaction reduces with increasing temperature for an aqueous solution of HA.[37] The shear modulus for collagen also decreases when increasing temperature.[38] The shear moduli of collagen, HA, and the vitreous (consisting of collagen and HA) scale with temperature. Therefore, the viscoelastic interaction that scales depending on temperature, affects mobility of the coated probes. The coating RDs are measured from a sample at a constant temperature with a coated probe and a control probe. The RD removes the scalable temperature effects and provides a measure of a relative mobility effect of a coating. Similar percentual effects as in the study are also expected in a higher temperature in the human vitreous (around 35–37 °C).[39] However, we can assume that the mobility of the enzymatically coated probes would be higher at human body temperature, because enzymatic activity is increased at higher temperatures. Furthermore, time-dependent effects of the enzymatic coatings are expected to happen faster at a higher temperature.

Hydrophilic Coatings. Figure 6 shows the mean and SeM values of |G| measured with the hydrophilic-polymer coated probes in collagen gel. The mean |G| values measured in ex vivo porcine vitreous are shown in Supporting Information (Figure S3). HA coating increases the mean |G| in both vitreous models, whereas all the other coatings (PEG, PVP, and TiO_2) decrease the mean |G| or have no significant effect. The |G| values measured with coated and control probes vary between each sample (Supporting Information, Figure S4) because of biovariation of the individual ex vivo porcine eyes and prepared collagen samples. Therefore, the mean |G| values include the individual variation of samples in addition to the potential coating effect. For example, there is no difference found between the mean |G| of the PEG coating and the control (Figure S3b); however, |G| of the coated probe is typically lower than the control in each experiment (Supporting Information, Figure S4). To study the coating effects independent of the variation of the individual samples, the mean RD values of the coatings were calculated.

The mean RD results from collagen gel (Figure 7a) and ex vivo porcine vitreous (Figure 7b) indicate increased mobility for PEG (collagen n = 3; vitreous n = 5), PVP (collagen n = 5; vitreous n = 7), and TiO_2 (collagen n = 3; vitreous n = 4) and decreased mobility for HA (collagen n = 4; vitreous n = 3). Qualitatively both vitreous models give similar results, however, the effect of the coating on the mean RD value is larger in collagen gel than in ex vivo porcine vitreous. On the basis of the results, the excitation frequency does not significantly change the performance of a coating. Therefore, the data obtained at different frequencies were pooled together for statistical analysis.

Enzyme Coatings. Figure 8 presents the results of the mean |G| from hyaluronidase- and collagenase-coated probes characterized in the vitreous models. Measurements were taken

DOI: 10.1021/acsami.5b06937
ACS Appl. Mater. Interfaces 2015, 7, 22018–22028

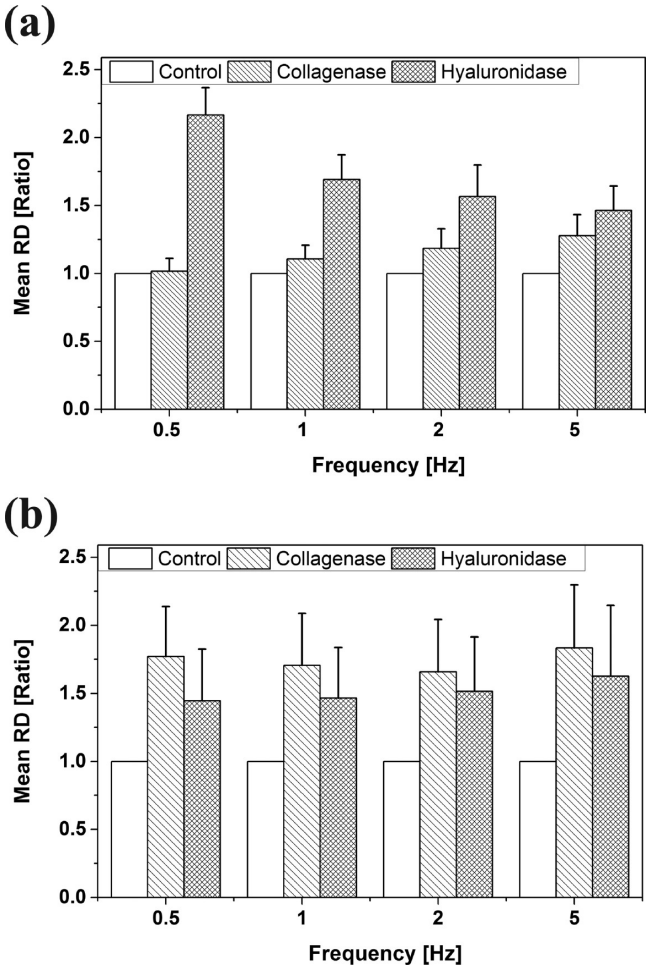

Figure 9. (a) The mean RD values for collagenase- and hyaluronidase-coated probes in collagen and HA gel, respectively. (b) The mean RD values for collagenase- and hyaluronidase-coated probes in ex vivo porcine vitreous.

after the probes were in contact with the vitreous sample for 5 min. Figure 9 presents the mean RDs of the data. The

Table 4. Statistical Significance of the Coatings Affecting Mobility in In Vitro Samples[a]

coating	effect	n	p-value	adjusted p
PVP	increase	5	0.0058	0.0230
PEG	increase	3	< 0.0001	< 0.0001
HA	decrease	4	< 0.0001	< 0.0001
TiO_2	increase	3	0.0001	0.0004
collagenase	increase	8	0.0312	0.0312
hyaluronidase	increase	7	< 0.0001	< 0.0001

[a]PVP, PEG, HA, TiO_2 and collagenase coatings were characterized in collagen gel. Hyaluronidase was characterized in HA gel.

Table 5. Statistical Significance of the Coatings Affecting Mobility in Ex Vivo Porcine Vitreous

coating	effect	n	p-value	adjusted p
PVP	increase	7	0.4384	1.0000
PEG	increase	5	0.0811	0.3244
HA	decrease	3	0.0719	0.2876
TiO_2	increase	4	0.0057	0.0228
collagenase	increase	8	0.0003	0.0006
hyaluronidase	increase	6	0.0133	0.0266

hyaluronidase coating reduces the mean |G| in HA (n = 7) and in ex vivo porcine vitreous (n = 6). The mean RD increases compared to the controls in both cases (72.2% in HA, and 51.4% in ex vivo porcine vitreous). The mean RD of hyalurodinase-coated probes increases with increased duration in HA (20% increase within 15−20 min; n = 2) and in ex vivo porcine vitreous (11% increase within 15 min; n = 3). Hyaluronidase coating in HA (see Figure 9a) shows a decreasing trend of the mean RD with increasing probe excitation frequency. This can be caused by a decreased proportion of the viscosity-related loss modulus in the response (i.e., related to shearing with the coating) at higher shear rates.[9]

The collagenase coating has an insignificant effect on the mean |G| values measured in collagen gel. In this case, the effect of biovariation within the collagen samples may be more prominent than the potential coating effect in the mean |G|.

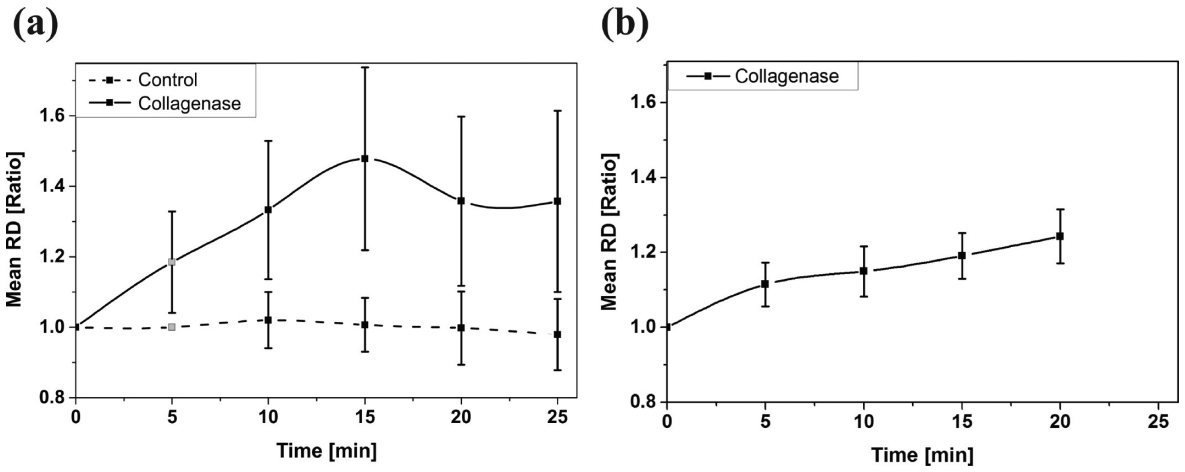

Figure 10. Collagenase coating: time-dependent mean RDs with SeMs in errorbars. (a) Time-dependent results in collagen (n = 9). The results indicated with gray dots are from the collagenase-coating experiments for 5 min (n = 8) shown for comparison. The experiments with coated probes and control probes were performed in two corresponding samples from the same collagen. (b) Time-dependent results in ex vivo porcine vitreous (n = 3). Control experiments in ex vivo porcine vitreous were not performed similarly as in (a), because any two ex vivo vitreous samples have individual differences. Hence, the initial displacement amplitude of the coated probe was considered as control ($x_{\text{control}}^{\text{amplitude}}$).

DOI: 10.1021/acsami.5b06937
ACS Appl. Mater. Interfaces 2015, 7, 22018−22028

The measured |G| is typically lower for collagenase than for the controls in each sample (Supporting Information, Figure S5). Collagenase increased the mean RD by 14.6% (n = 8) in collagen gel. A potential increase of the mean RD at higher frequencies (Figure 9a) could be explained by an enhanced interaction of collagenase with the collagen. In ex vivo porcine vitreous, collagenase has a reducing effect to the mean |G|, and the mean RD is increased by 74.2% (n = 8). A potential reason for collagenase affecting less in collagen gel than in ex vivo porcine vitreous is that it did not have sufficient time for enzymatic digestion of collagen with the used collagen concentration (used collagen 5 mg/mL, the collagen in the vitreous 300 μg/mL[21]). Figure 10 presents time-dependent mean RD results for the collagenase coating with smoothing spline fits to illustrate the trends. There was a significant increase in the mean RD of collagenase-coated probes in collagen gel with increased duration ≥10 min (48% increase from the initial displacement after 15 min; n = 9). The mean RD in ex vivo porcine vitreous also increased with increased duration (19% increase from the initial displacement after 15 min; n = 3).

Statistical Analysis. Figure S6 (Supporting Information) illustrates the extent of the change in mobility affected by the hydrophilic coatings. TiO_2 improves mobility significantly based on the increased mean RDs in both collagen gel and in ex vivo porcine vitreous models (Tables 4 and 5). PVP and PEG increase the mean RD significantly in collagen gel. Their mobility increase in the vitreous is insignificant at 95% CL; however, the increasing trend is similar to that of collagen gel (increased mean RDs; Figure S6). The hydrophilic nature of these polymers and prevention of protein adsorption are potential reasons for the mobility improvement.[15] HA decreases the mean RD in collagen gel significantly, however, the decrease in the vitreous is insignificant at 95% CL. The reason for HA decreasing mobility could be a high number of oxygen molecules in HA structure which could bind with the vitreal macromolecules (i.e., HA, collagen, proteoglycans) or water via hydrogen bonds.

In the experiments with enzymatic exposure of 5 min in the vitreous, statistical analysis of the mean RD was performed for the average effect where the data at all frequencies were pooled together. Hyaluronidase improves the mean RD in ex vivo porcine vitreous and in HA gel. In similar experiments, collagenase also improves the mean RD significantly in ex vivo porcine vitreous and in collagen gel (Tables 4 and 5). Both hyaluronidase and collagenase increase mobility with time during 10 to 25 min tests.

CONCLUSION

Developing surgical microdevices to operate in the vitreous involve challenges regarding nonlinear hindered mobility in the ocular vitreous. Hydrophilic coatings have the potential to improve mobility by reducing the biomolecular adsorption partially responsible for hindered movement. Enzymes are another group of potential microdevice coatings that can be used to facilitate movement through the liquification of surrounding biomolecules. Four hydrophilic coatings (PEG, PVP, HA, TiO_2) and two enzymatic coatings (collagenase and hyaluronidase) were prepared and applied on probes modeling surgical devices. The mobility of the coatings was characterized by oscillatory magnetic microrheology in ex vivo porcine vitreous, synthesized collagen gel, and HA gel.

All studied hydrophilic coatings improve mobility (i.e., the mean RD increased, and the mean |G| decreased or stayed the same), except for HA coating which decreases mobility potentially due to chemical interactions with vitreal macromolecules. The coatings cause comparable effects in collagen gel and in ex vivo porcine vitreous; however, the effects are lower in the vitreous that can be due to a lower concentration of collagen in the vitreous than in the prepared collagen samples. The calculated mean |G| values reflect coating-dependent effects, however, they are also be affected by individual vitreous differences. The |G| values of the controls are consistent with the literature. The mean RD values are calculated based on |G| data. Statistical analysis was performed based on the mean RD values, which are not sensitive to the individual vitreous differences. TiO_2 coating significantly improves the mean RD in collagen gel by 28.3% and in ex vivo porcine vitreous by 15.4%. PEG and PVP coatings significantly improve the mean RD in collagen gel by 19.4 and by 39.6%, respectively. The mean RD improvement of PEG and PVP coatings in ex vivo porcine vitreous is insignificant at 95% CL. HA coating reduces mobility in collagen gel (by 35.6%), but the decrease in ex vivo porcine vitreous is insignificant at 95% CL.

Enzymatic coatings of collagenase and hyaluronidase increase the mean RD more than the hydrophilic coatings (i.e., > 40% after experiments with 15 min duration in the vitreous models). However, the enzymes have time-dependent effects and they dissolve from the probe surface with time. In the experiments with enzymatic exposure of 5 min, hyaluronidase significantly improved the mean RD in ex vivo porcine vitreous (by 51.4%) and in HA (by 72.2%). Collagenase significantly improved the mean RD in ex vivo porcine vitreous (by 74.2%) and in collagen gel (by 14.6%). Both collagenase and hyaluronidase result in time-dependent mobility improvements in the vitreous models.

These results are useful for researchers working to enhance the mobility of devices in the human eye vitreous for surgical procedures. They also pave the way for understanding how to adjust mobility in complex fluids by choosing an appropriate coating.

ASSOCIATED CONTENT

Supporting Information

The Supporting Information is available free of charge on the ACS Publications website at DOI: 10.1021/acsami.5b06937.

Preparation of collagen among the vitreous models (i.e., for characterization of collagen gel polymerization time), characterization of the setup for oscillatory microrheology, and shear modulus and RD results related to mobility. (PDF)

AUTHOR INFORMATION

Corresponding Authors

*E-mail: juho.pokki@gmail.com.
*E-mail: vidalp@ethz.ch.

Notes

The authors declare no competing financial interest.

ACKNOWLEDGMENTS

This research was supported by the European Research Council Advanced Grant BOTMED. We acknowledge Dr. Mahmut Selman Sakar, Alexander Tanno, Dr. Stefano Fusco, Berna

DOI: 10.1021/acsami.5b06937
ACS Appl. Mater. Interfaces 2015, 7, 22018−22028

Özkale, Jiaming Yang, Simone Gervasoni, Norman Pedrini, and Fajer Mushtaq. We thank SuSoS AG for developing the recipes of three hydrophilic coatings. M.G. acknowledges the support of the Secretary for Universities and Research of the Government of Catalonia and the COFUND Programme of the Marie Curie Actions of the seventh R&D Framework Programme of the European Union for the "Beatriu de Pinos" contract (2013 BP-B 00077).

REFERENCES

(1) Wong, Y. H. I.; Cheung, N. D.; Wong, D. S. H. *Vitreous in Health and Disease*; Springer: New York, 2014.
(2) Kirchhof, B.; Wong, D. *Vitreo-Retinal Surgery*; Springer: New York, 2007.
(3) Peyman, G.; Meffert, S.; Chou, F.; Conway, M. *Vitreoretinal Surgical Techniques*; Taylor & Francis: Abingdon, U.K., 2000.
(4) Alfaro, D.; Liggett, P. *Vitreoretinal Surgery of the Injured Eye*; Lippincott-Raven: Philadelphia, PA, 1999.
(5) Friedman, D. S.; O'Colmain, B. J.; Munoz, B.; Tomany, S. C.; McCarty, C.; De Jong, P. T.; Nemesure, B.; Mitchell, P.; Kempen, J. Prevalence of Age-Related Macular Degeneration in the United States. *Arch. Ophthalmol.* **2004**, *122*, 564−572.
(6) Saaddine, J. B.; Honeycutt, A. A.; Narayan, K. V.; Zhang, X.; Klein, R.; Boyle, J. P. Projection of Diabetic Retinopathy and Other Major Eye Diseases among People with Diabetes Mellitus: United States, 2005−2050. *Arch. Ophthalmol.* **2008**, *126*, 1740−1747.
(7) Stalmans, P.; Girach, A. Vitreous Levels of Active Ocriplasmin Following Intravitreal Injection: Results of an Ascending Exposure Trial. *Invest. Ophthalmol. Visual Sci.* **2013**, *54*, 6620−6627.
(8) Nelson, B. J.; Kaliakatsos, I. K.; Abbott, J. J. Microrobots for Minimally Invasive Medicine. *Annu. Rev. Biomed. Eng.* **2010**, *12*, 55−85.
(9) Sharif-Kashani, P.; Hubschman, J.-P.; Sassoon, D.; Pirouz Kavehpour, H. Rheology of the Vitreous Gel: Effects of Macromolecule Organization on the Viscoelastic Properties. *J. Biomech* **2011**, *44*, 419−423.
(10) Pokki, J.; Ergeneman, O.; Sevim, S.; Enzmann, V.; Torun, H.; Nelson, B. J. Measuring Localized Viscoelasticity of the Vitreous Body using Intraocular Microprobes. *Biomed. Microdevices* **2015**, *17*, 1−9.
(11) Filas, B. A.; Zhang, Q.; Okamoto, R. J.; Shui, Y.-B.; Beebe, D. C. Enzymatic Degradation Identifies Components Responsible for the Structural Properties of the Vitreous Body. *Invest. Ophthalmol. Visual Sci.* **2014**, *55*, 55−63.
(12) He, J.; Tang, J. X. Surface Adsorption and Hopping Cause Probe-Size-Dependent Microrheology of Actin Networks. *Phys. Rev. E* **2011**, *83*, 041902.
(13) Wang, Z.; Pokki, J.; Ergeneman, O.; Nelson, B. J.; Hirai, S. Viscoelastic Interaction between Intraocular Microrobots and Vitreous Humor: A Finite Element Approach. *In Proc. IEEE EMBC* **2013**, 4937−4940.
(14) Lu, Q.; Solomon, M. J. Probe Size Effects on the Microrheology of Associating Polymer Solutions. *Phys. Rev. E: Stat. Phys., Plasmas, Fluids, Relat. Interdiscip. Top.* **2002**, *66*, 061504.
(15) Serrano, Â.; Sterner, O.; Mieszkin, S.; Zürcher, S.; Tosatti, S.; Callow, M. E.; Callow, J. A.; Spencer, N. D. Nonfouling Response of Hydrophilic Uncharged Polymers. *Adv. Funct. Mater.* **2013**, *23*, 5706−5718.
(16) Rabe, M.; Verdes, D.; Seeger, S. Understanding protein adsorption phenomena at solid surfaces. *Adv. Colloid Interface Sci.* **2011**, *162*, 87−106.
(17) Waigh, T. A. Microrheology of Complex Fluids. *Rep. Prog. Phys.* **2005**, *68*, 685.
(18) Williams, G. 25-, 23-, or 20-Gauge Instrumentation for Vitreous surgery? *Eye* **2008**, *22*, 1263−1266.
(19) Lee, B.; Litt, M.; Buchsbaum, G. Rheology of the Vitreous Body. Part I: Viscoelasticity of Human Vitreous. *Biorheology* **1992**, *29*, 521−533.
(20) Lee, B.; Litt, M.; Buchsbaum, G. Rheology of the Vitreous Body. Part 2: Viscoelasticity of Bovine and Porcine Vitreous. *Biorheology* **1994**, *31*, 327−338.
(21) Balazs, E. A. In *Physiology of the Vitreous Body*; Schepens, C., Ed.; CV Mosby: St. Louis, MO, 1960; pp 29−57.
(22) Bishop, P. N. Structural Macromolecules and Supramolecular Organisation of the Vitreous Gel. *Prog. Retinal Eye Res.* **2000**, *19*, 323−344.
(23) Rajan, N.; Habermehl, J.; Cote, M.-F.; Doillon, C. J.; Mantovani, D. Preparation of Ready-to-Use, Storable and Reconstituted Type I Collagen from Rat Tail Tendon for Tissue Engineering Applications. *Nat. Protocols* **2007**, *1*, 2753−2758.
(24) Nickerson, C. S. Engineering the Mechanical Properties of Ocular Tissues. Ph.D. thesis, Caltech: Pasadena, CA, 2006.
(25) Sebag, J. Ageing of the Vitreous. *Eye* **1987**, *1*, 254−262.
(26) Han, W.; Wang, Y. D.; Zheng, Y. F. In Vivo Biocompatibility Studies of Nano TiO_2 Materials. *Adv. Mater. Res.* **2009**, *79*, 389−392.
(27) Guerrero, M.; Altube, A.; García-Lecina, E.; Rossinyol, E.; Baró, M. D.; Pellicer, E.; Sort, J. Facile In Situ Synthesis of BiOCl Nanoplates Stacked to Highly Porous TiO_2: A Synergistic Combination for Environmental Remediation. *ACS Appl. Mater. Interfaces* **2014**, *6*, 13994−14000.
(28) Musić, S.; Gotić, M.; Ivanda, M.; Popović, S.; Turković, A.; Trojko, R.; Sekulić, A.; Furić, K. Chemical and Micro Structural Properties of TiO_2 Synthesized by Sol-Gel Procedure. *Mater. Sci. Eng., B* **1997**, *47*, 33−40.
(29) Djaoued, Y.; Badilescu, S.; Ashrit, P.; Bersani, D.; Lottici, P.; Brüning, R. Low Temperature Sol-Gel Preparation of Nanocrystalline TiO_2 Thin Films. *J. Sol-Gel Sci. Technol.* **2002**, *24*, 247−254.
(30) Mano, S. S.; Kanehira, K.; Sonezaki, S.; Taniguchi, A. Effect of Polyethylene Glycol Modification of TiO_2 Nanoparticles on Cytotoxicity and Gene Expressions in Human Cell Lines. *Int. J. Mol. Sci.* **2012**, *13*, 3703−3717.
(31) Nanci, A.; Wuest, J.; Peru, L.; Brunet, P.; Sharma, V.; Zalzal, S.; McKee, M. Chemical Modification of Titanium Surfaces for Covalent Attachment of Biological Molecules. *J. Biomed. Mater. Res.* **1998**, *40*, 324−335.
(32) Brena, B.; González-Pombo, P.; Batista-Viera, F. *Immobilization of Enzymes and Cells*; Springer: New York, 2013; pp 15−31.
(33) Nisha, S.; Arun, K. S.; Gobi, N. A Review on Methods, Application and Properties of Immobilized Enzyme. *Che. Sci. Rev. Lett.* **2012**, 148−155.
(34) McCormack, J.; Vandermeer, B.; Allan, G. M. How Confidence Intervals Become Confusion Intervals. *BMC Med. Res. Methodol.* **2013**, *13*, 134.
(35) Knapp, D. M.; Barocas, V. H.; Moon, A. G.; Yoo, K.; Petzold, L. R.; Tranquillo, R. T. Rheology of Reconstituted Type I Collagen Gel in Confined Compression. *J. Rheol.* **1997**, *41*, 971−993.
(36) Wu, C.-C.; Ding, S.-J.; Wang, Y.-H.; Tang, M.-J.; Chang, H.-C. Mechanical Properties of Collagen Gels Derived from Rats of Different Ages. *J. Biomater. Sci., Polym. Ed.* **2005**, *16*, 1261−1275.
(37) Rwei, S.-P.; Chen, S.-W.; Mao, C.-F.; Fang, H.-W. Viscoelasticity and Wearability of Hyaluronate Solutions. *Biochem. Eng. J.* **2008**, *40*, 211−217.
(38) Velegol, D.; Lanni, F. Cell Traction Forces on Soft Biomaterials. I. Microrheology of Type I Collagen Gels. *Biophys. J.* **2001**, *81*, 1786−1792.
(39) Ooi, E.; Ang, W.-T.; Ng, E. Bioheat Transfer in the Human Eye: A Boundary Element Approach. *Eng. Anal. Bound. Elem.* **2007**, *31*, 494−500.

DOI: 10.1021/acsami.5b06937
ACS Appl. Mater. Interfaces 2015, 7, 22018−22028